Intra- and inter-multiplet magnetic excitations in a tetrairon(III) molecular cluster

S. Carretta, P. Santini, and G. Amoretti
Istituto Nazionale per la Fisica della Materia, Dipartimento di Fisica, Università di Parma, I-43100 Parma, Italy

T. Guidi and R. Caciuffo
Istituto Nazionale per la Fisica della Materia, Dipartimento di Fisica ed Ingegneria dei Materiali, Università Politecnica delle Marche, I-60131 Ancona, Italy

A. Candini
INFM-S^3 National Research Center, Dipartimento di Fisica, Università di Modena e Reggio Emilia, I-41100 Modena, Italy

A. Cornia
Dipartimento di Chimica-Centro SCS, Università di Modena e Reggio Emilia, UdR INSTM, Via G. Campi 183, I-41100 Modena, Italy

D. Gatteschi
Dipartimento di Chimica, Università di Firenze, I-50019 Sesto Fiorentino, Italy

M. Plazanet and J. A. Stride
Institut Laue Langevin, Boîte Postale 220 X, F-38042 Grenoble Cedex, France
(Received 31 May 2004; published 2 December 2004)

We used inelastic neutron scattering to determine the microscopic spin Hamiltonian of a tetrairon(III) molecular cluster with trigonal symmetry, $[Fe_4(thme)_2(dpm)_6]$, obtained from a parent compound with C_2 symmetry by site-specific ligand substitution. Intra-multiplet excitations within the anisotropy split $S=5$ ground spin state, and inter-multiplet transitions toward the first $S=4$ excited states have been observed. The model spin Hamiltonian used to interpret the experimental data evidences an enhancement of the anisotropy barrier due to the chemical modification of the parent molecular cluster. A rhombic anisotropy term, forbidden in D_3 symmetry, is necessary to reproduce experimental data. The determination of this term is crucial for the understanding of quantum tunneling of the magnetization in this model compound. The calculated temperature dependence of heat capacity for different applied magnetic field values is in good agreement with experimental measurements. Within this model, the estimated temperature dependence of the relaxation time agrees with available experimental data.

DOI: 10.1103/PhysRevB.70.214403 PACS number(s): 75.50.Tt, 75.10.Jm, 75.40.Gb, 75.45.+j

I. INTRODUCTION

The most promising feature that makes molecular nanomagnets (MNM) interesting for technological applications, in particular for information storage, is the magnetic bistability they exhibit at low temperature. This behavior, first observed in a Mn12 cluster,[1] is determined by the anisotropy barrier hindering the reversal of the magnetization. Considerable efforts have been devoted to the attempt to increase the barrier height and, consequently, the blocking temperatures in order to make real applications viable. MNM are clusters of exchange-coupled transition-metal ions and the height of the magnetic anisotropy barrier is mainly associated with the total spin value in the ground state and with the sum of single-ion anisotropies, which in turn are dependent on the nature of the ligands and their arrangement around the metal centers. Dipole-dipole interactions and mixing of states with different total spin can also play an important role[2] and must usually be taken into account.

Several compounds with large values of the total spin have already been synthesized,[3] but the control of the anisotropy by site-specific chemical substitutions turned out to be a difficult task. Nevertheless, this remains a major goal of synthetic chemistry research. Recently, replacement of six methoxide bridges with two triply-deprotonated 1,1,1-tris(hydroxymethyl)ethane H_3thme ligands in a preformed $[Fe_4(OMe)_6(dpm)_6]$ (briefly Fe_4-OMe) cluster yielded a novel variety, that crystallizes in a trigonal lattice, $[Fe_4(thme)_2(dpm)_6]$ (briefly Fe_4-thme, Hdpm =dipivaloylmethane).[4] The structure of this molecule is characterized by a symmetry higher than that of the parent compound (see Fig. 1): three iron(III) ions lie at the vertices of an equilateral triangle, with the fourth at the center, raising the symmetry from C_2 to D_3. The random disorder in the coordination environment of the Fe2 and Fe2' ions, that in the parent compound leads to the coexistence of three isomers in the crystal lattice,[5] is not observed here and the system is highly ordered. High-frequency electron paramagnetic resonance (HF-EPR) spectra revealed a doubling of the magnetic anisotropy in the $S=5$ spin ground state, and magnetic relaxation measurements have shown more than a fourfold increase in the activation energy for magnetization reversal.[4] The small dimension of the Hilbert space and the presence of a single isomer make Fe_4-thme a model compound for studying quantum tunneling of the magnetization (QTM) phenomena in detail.

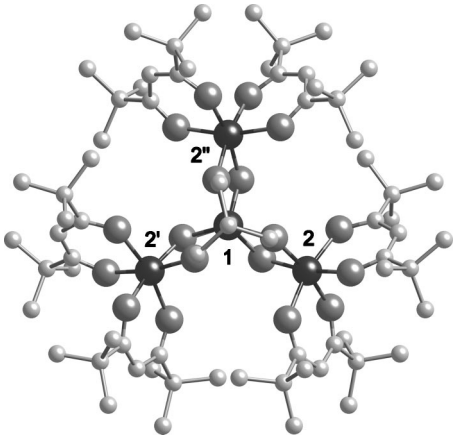

FIG. 1. Molecular structure of the Fe_4-thme cluster. The four iron(III) ions are represented by large dark circles; the oxygen and carbon atoms are large and small gray circles, respectively. Hydrogen atoms are omitted for clarity.

Here, we report the results of inelastic neutron scattering (INS) experiments on a deuterated polycrystalline sample of Fe_4-thme. Their interpretation in terms of an effective spin Hamiltonian including exchange, crystal-field, and dipole-dipole interactions allows us to determine the values of the intra-cluster exchange integrals, the zero-field-splitting (ZFS) parameters up to the fourth order, and the composition of the spin wave functions. The ZFS parameters compare favorably with those deduced from HF-EPR spectra, but nonzero values of the rhombic and fourth-order terms are needed to obtain a good fitting of the neutron data. The determination of in-plane anisotropy terms is crucial to understand quantum tunneling of the magnetization in this model compound. The proposed energy level scheme is used to calculate the magnetic field dependence of the Fe_4-thme heat capacity in the temperature range from 2 to 20 K, and excellent agreement with experimental data is obtained.

By means of a master equation approach, we have calculated the temperature dependence of the relaxation time τ of the magnetization. Results are discussed in Sec. III.

II. EXPERIMENTAL DETAILS

For the neutron experiments, we used 1.3 g of deuterated microcrystalline Fe_4-thme. The procedure outlined in Ref. 6 was adapted to the large-scale preparation of d_{18}-Hdpm from acetone-d_6. Variations include the use of nondeuterated sulfuric acid for the transposition of pinacol-d_{14} (Ref. 7) to pinacolone-d_{12},[8] which was subsequently converted to trimethyl-d_9-acetic acid.[9] Treatment of the latter with $SOCl_2$ gave crude trimethyl-d_9-acetylchloride, which was directly converted to methyl trimethyl-d_9-acetate by a standard method.[10] Distilled methyl trimethyl-d_9-acetate was finally reacted with pinacolone-d_{12} and NaH in dimethoxyethane[11] to give d_{18}-Hdpm, which was purified by distillation. Starting from 87.2 g of acetone-d_6, we obtained 8.24 g of pure d_{18}-Hdpm (b.p. 71–73 °C at 7 mmHg). The isotopic purity, determined utilizing ^{1}H NMR, was 98 at. % D. The dimer $[Fe_2(OMe)_2(d_{18}\text{-dpm})_4]$ was synthesized using the deuterated ligand and reacted with appropriate amounts of $FeCl_3$ and NaOMe in a $MeOH/Et_2O$ solvent mixture as described in Ref. 4. After removal of NaCl by filtration, the yellow solution was layered with a solution of H_3thme (3 equiv.) in $MeOH/Et_2O$ 1:9 (v/v) and left undisturbed for 10 days. The yellow prisms of $[Fe_4(thme)_2(d_{18}\text{-dpm})_6]$ so obtained were collected by filtration, washed with MeOH, and dried under vacuum. Based on the total amount of iron used, the yield was as high as 57%, to be compared with 42–49 % for the two-step procedure previously reported.[4] Since the $thme^{3-}$ ligands were not isotopically enriched, the isotopic purity of the sample amounted to ~80 at. % D (this value was not checked, as *tert*-butyl groups do not undergo H-D exchange in the adopted experimental conditions). X-ray diffraction analysis showed that all the observed Bragg peaks could be indexed in the $R\bar{3}c$ space group, with the same lattice parameters reported for the nondeuterated variant.[4] Structural details are reported in Ref. 4. The molecule exhibits D_3 symmetry, with the C_3 axis perpendicular to the plane of the equilateral triangle (Fe1-Fe2 = 3.086 Å).

INS measurements have been performed at the Institute Laue-Langevin in Grenoble (France), with the time-of-flight spectrometers IN4 and IN5. On the first instrument, neutrons with incident wavelength $\lambda = 1.8$ Å were used to collect data in the energy-transfer range up to 20 meV, with a resolution of 0.77 meV at the elastic peak. On IN5, neutrons with incident wavelength $\lambda = 8.5$ Å have been used to explore the energy-transfer range from −0.6 to 0.6 meV, with a resolution better than 25 μeV. The first set of measurements was performed to observe inter-multiplet excitations and determine the intra-cluster exchange integrals. The aim of the second experiment was to determine energy and intensities of transitions between the components of the anisotropy-split $S=5$ ground state. The sample was placed in a hollow aluminum cylinder (0.7 mm wall thickness, 20 mm inner diameter), and inserted into a standard ILL cryostat allowing the sample to be cooled down to 2 K. Standard data treatments have been performed, using a vanadium sample for calibration.

Specific-heat measurements have been carried out on a small amount of the sample used for the INS experiments. A 5-mg compact specimen was prepared by pressing Fe_4-thme microcrystals without any additive. Data have been collected using the relaxation method as a function of temperature and magnetic field amplitude, using a PPMS-7 Quantum Design platform.

III. RESULTS AND DISCUSSION

For large values of the momentum transfer Q, the INS response is dominated by vibrational, multiphonon, and multiple-phonon contributions. However, by following the Q dependence of their intensity, nondispersive magnetic excitations can be safely identified. Figure 2 shows the sum of the raw spectra recorded at $T=2$ K by the IN4 detectors covering the angle range from 13.1 to 31.6 degrees.

The peaks emerging from the background at about 5.7 and 12 meV are attributed to transitions from the $S=5$ ground state to excited spin states. Indeed, assuming isotropic

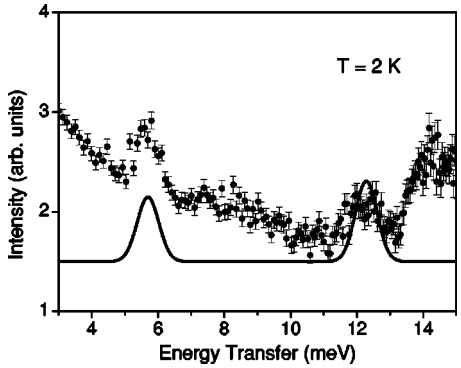

FIG. 2. INS spectra recorded on IN4 using an incident wavelength $\lambda = 1.8$ Å, with the sample kept at 2 K. The displayed intensity results from the integration over a limited interval of Q, corresponding to scattering angles ranging from 13.1 to 31.6 degrees. The two Gaussian line shapes represent calculated transitions, under the hypothesis of isotropic exchange interaction with parameters given in the text.

Heisenberg exchange interactions ($H_{\text{exch}} = \Sigma_{i>j} J_{ij} \mathbf{s}_i \cdot \mathbf{s}_j$), and the nearest-neighbor and next-nearest-neighbor constants that fit the magnetic susceptibility curve,[4] $J_{12} = 2.05(1)$ meV (antiferromagnetic) and $J_{22'} = -0.08(1)$ meV (ferromagnetic), the energy level scheme reported in Fig. 3 is obtained. In the preceding formula, $\mathbf{s}_i$ and $\mathbf{s}_j$ are local spin operators. The D_3 symmetry of the exchange interactions allows us to diagonalize analytically the Heisenberg Hamiltonian. In particular, by choosing the successive coupling scheme ($S_{2,2'} = s_2 + s_{2'}$, $S_{\text{ext}} = S_{2,2'} + s_{2''}$, and $S = S_{\text{ext}} + s_1$), one obtains

$$E(S, S_{\text{ext}}) = \frac{J_{12}}{2} S(S+1) + \frac{J_{22'} - J_{12}}{2} S_{\text{ext}}(S_{\text{ext}} + 1). \qquad (1)$$

Since, in this symmetry, the energy does not depend on $S_{2,2'}$, many multiplets are degenerate (e.g., the two lowest $S = 4$ multiplets at 5.7 meV). The observed peaks would therefore correspond to the $S = 5$ ($S_{\text{ext}} = 15/2$) $\rightarrow S = 4$ ($S_{\text{ext}} = 13/2$) transition and to the $S = 5 \rightarrow S = 6$ ($S_{\text{ext}} = 15/2$) transition predicted at 12.2 meV. The corresponding calculated intensities are shown in Fig. 2 as Gaussian line shapes with full

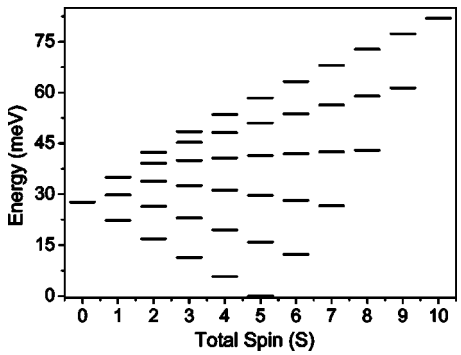

FIG. 3. Energy of the lowest eigenstates as a function of the total spin S calculated for the Fe_4-thme cluster assuming isotropic exchange interactions only, with parameters $J_{12} = 2.05(1)$ meV and $J_{22'} = -0.08(1)$ meV.

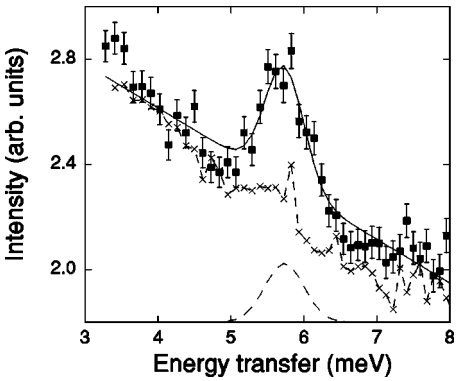

FIG. 4. The magnetic excitation between the $S = 5$ ground state and the two degenerate lowest-energy $S = 4$ multiplets. Data have been fitted assuming a sloping background under a single Gaussian peak with FWHM close to the instrumental resolution (FWHM = 0.77 meV). Crosses represent intensities measured at high scattering angle (from 106.2 to 120.3 degrees), scaled at the value observed at low angle and 3 meV energy transfer.

width at half maximum (FWHM) equal to the instrument resolution (0.77 meV) and height proportional to the transition probability. A fit of the measured intensities is not attempted, because of the difficulty of subtracting reliably the nonmagnetic background.

The $S = 4$ multiplet at 5.7 meV is twofold-degenerate. A departure from trigonal symmetry would lift this degeneracy, and would require a larger number of different exchange integrals to be considered. Since the experimental peak (Fig. 4) is excellently reproduced by a single Gaussian having a FWHM equal to the instrumental resolution, no evidence of symmetry lowering is found. This result can be compared with that obtained with similar experiments for the parent compound Fe_4-OMe. In that case, the degeneracy of the first-excited $S = 4$ states is clearly lifted, as two peaks appear in the INS cross section at 7.3 and 8.3 meV.[12] A simultaneous fitting of INS intensity and magnetic susceptibility gave $J_{12} = J_{12'} = 2.8$ meV, $J_{12''} = 2.3$ meV, and $J_{22'} = J_{22''} = J_{2'2''} = -0.15$ meV.

The $(2S+1)$-fold degeneracy of each S multiplet is removed by crystal field and anisotropic intra-cluster spin-spin interactions,

$$H_{\text{ZFS}} = \sum_i \sum_{k,q} b_k^q(i) O_k^q(\mathbf{s}_i) + \sum_{i>j} \mathbf{s}_i \cdot \mathbf{D}_{ij} \cdot \mathbf{s}_j, \qquad (2)$$

where $O_k^q(\mathbf{s}_i)$ are Stevens operator equivalents for the ith ion[13] of the cluster. The anisotropic splitting of the $S = 5$ ground state can be observed by high-resolution INS experiments. Figure 5 shows the spectra recorded on IN5, with the sample kept at 2 and 11 K. At the lowest temperature, a single sharp peak at 0.49 meV is observed. Assuming easy axis anisotropy, this peak must correspond to the $|S = 5, M = \pm 5\rangle \rightarrow |S = 5, M = \pm 4\rangle$ transition, as only the lowest doublet is thermally populated at $T = 2$ K. Increasing the temperature to 11 K, all the components of the anisotropy split $S = 5$ state become populated, allowing the transitions between them to be visible.

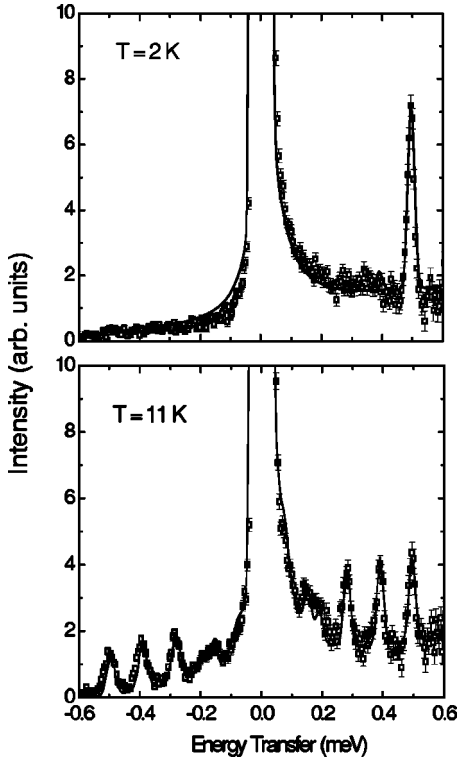

FIG. 5. INS spectra collected with $\lambda = 8.5$ Å and $T = 2$ K (top) and $T = 11$ K (bottom). Solid lines represent the spectra calculated from eigenvalues and eigenvectors of the ZFS Hamiltonian given in the text, by associating to each transition a Gaussian line shape with a height proportional to the calculated probability and a width of 25 μeV, corresponding to the experimental resolution. The elastic peak and a quasielastic contribution have been included in the best-fit procedure.

In the strong-exchange limit, the ZFS term can be introduced as a perturbation to the dominant isotropic exchange interaction and can be projected over the total spin subspaces. Hereafter, we assume that the z axis is directed along the C_3 symmetry axis. Limiting our discussion to the ground state, and assuming D_3 symmetry, we should therefore write

$$H_{\mathrm{ZFS}}^{(D_3)} = B_2^0 \hat{O}_2^0 + B_4^0 \hat{O}_4^0 + B_4^3 \hat{O}_4^3, \tag{3}$$

where B_n^m are anisotropy parameters and $\hat{O}_n^m$ are Stevens operator equivalents defined in the space of the $S=5$ multiplet, i.e.,

$$\hat{O}_2^0 = 3S_z^2 - S(S+1),$$

$$\hat{O}_4^0 = 35S_z^4 - [30S(S+1) - 25]S_z^2 - 6S(S+1) + 3S^2(S+1)^2,$$

$$\hat{O}_4^3 = \frac{S_z(S_+^3 + S_-^3) + (S_+^3 + S_-^3)S_z}{4}. \tag{4}$$

Diagonalization of the spin Hamiltonian $H_{\mathrm{ZFS}}^{(D_3)}$ gives eigenvalues and eigenvectors from which INS intensities can be calculated, following the procedure reported, for instance, in Ref. 14. The parameters of the Hamiltonian can therefore be determined from the experimental data by a best-fit procedure. We find that the Hamiltonian given by Eq. (3) does not lead to a satisfactory reproduction of the observed spectra, in particular below 0.3 meV, where the response is more sensitive to the mixing of $|M\rangle$ states produced by the nondiagonal terms in H_{ZFS}. On the other hand, as shown by solid lines in Fig. 5, an excellent fit is obtained by adding a rhombic term to $H_{\mathrm{ZFS}}^{(D_3)}$, and assuming

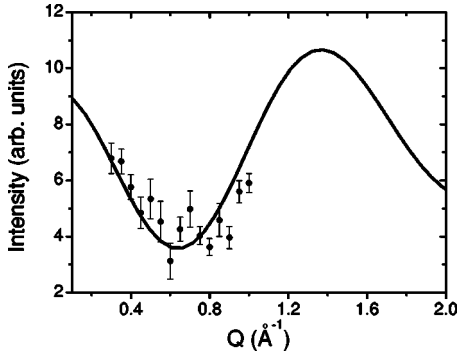

FIG. 6. INS intensity of the 0.49 meV peak as a function of the transferred wave vector Q. Data have been obtained on IN5 with incident wavelength $\lambda = 8.5$ Å and sample temperature $T = 2$ K. The solid line represents the curve calculated for the Hamiltonian given in the text.

$$H_{\mathrm{ZFS}} = H_{\mathrm{ZFS}}^{(D_3)} + B_2^2 \frac{S_+^2 + S_-^2}{2}. \tag{5}$$

This assumption implies that exact threefold symmetry is not achieved and that the iron triangle is not equilateral.

The results of the best-fit procedure give $B_2^0 = -18.6(4)$ μeV, $|B_2^2| = 1.2(6)$ μeV, and $B_4^0 = 1.0(5) \times 10^{-3}$ μeV, with a negligible $\hat{O}_4^3$ contribution ($|B_4^3| < \sim 0.1$ μeV). With these parameters and the atomic coordinates reported in Ref. 4, the Q dependence of the $|S=5, M=\pm 5\rangle \rightarrow |S=5, M=\pm 4\rangle$ transition can be evaluated using the formula for the INS cross section from a polycrystalline sample given in Ref. 15. The result of this calculation is compared with experiments in Fig. 6.

The B_2^0 parameter ($D/3$ in the conventional notation for the ZFS second-order tensor) is very close to the HF-EPR estimate and is more than twice as large as in the parent compound Fe_4-OMe, while B_4^0 has a comparable value but the opposite sign.[16] Also the rhombic term B_2^2 (E in the conventional notation) has here a value about twice as small as that determined for the dominant isomer present in Fe_4-OMe. With the lack of a significant in-plane trigonal contribution (B_4^3) to the magnetic anisotropy, only the modulus of B_2^2 can be determined, since a change of sign of this parameter corresponds to a rotation of 90 degrees around the z axis. Eigenvalues and corresponding eigenfunctions of the split $S=5$ ground multiplet are reported in Table I.

To double-check the reliability of the obtained ZFS parameters, we measured the low-temperature heat capacity in the presence of a magnetic field with amplitude up to 5 T. In Fig. 7, we report the molar specific heat C of Fe_4-thme measured in the temperature range 2–20 K and normalized to the gas constant R. The continuous lines in Fig. 7 are the

TABLE I. Eigenvalues (in meV units) and main contributions to the corresponding eigenvectors of the ground $S=5$ multiplet of Fe_4 evaluated with the best-fit parameters given in the text. The energy of the lowest doublet was set to zero.

Energy (meV)	State (main contributions)
0	$0.7085\|M=-5\rangle-0.7056\|M=5\rangle-0.0064\|M=-3\rangle+0.0064\|M=3\rangle$
0	$0.7056\|M=-5\rangle+0.7085\|M=5\rangle-0.0064\|M=-3\rangle-0.0064\|M=3\rangle$
0.497	$0.7070\|M=-4\rangle+0.7070\|M=4\rangle-0.0131\|M=-2\rangle-0.0131\|M=2\rangle$
0.497	$0.7070\|M=-4\rangle-0.7070\|M=4\rangle-0.0131\|M=-2\rangle+0.0131\|M=2\rangle$
0.8873	$-0.0064\|M=-5\rangle+0.0064\|M=5\rangle-0.7066\|M=-3\rangle+0.7066\|M=3\rangle$ $+0.0254\|M=-1\rangle-0.0254\|M=1\rangle$
0.8874	$0.0064\|M=-5\rangle+0.0064\|M=5\rangle+0.7066\|M=-3\rangle+0.7066\|M=3\rangle$ $-0.0254\|M=-1\rangle-0.0254\|M=1\rangle$
1.1665	$0.0131\|M=-4\rangle+0.0131\|M=4\rangle+0.7029\|M=-2\rangle+0.7029\|M=2\rangle$ $-0.1070\|M=0\rangle$
1.1692	$0.0131\|M=-4\rangle-0.0131\|M=4\rangle+0.7070\|M=-2\rangle-0.7070\|M=2\rangle$
1.321	$0.0254\|M=-3\rangle-0.0254\|M=3\rangle+0.7067\|M=-1\rangle-0.7067\|M=1\rangle$
1.3569	$0.0234\|M=-3\rangle+0.0234\|M=3\rangle+0.7067\|M=-1\rangle+0.7067\|M=1\rangle$
1.3977	$0.001\|M=-4\rangle+0.001\|M=4\rangle+0.0756\|M=-2\rangle+0.0756\|M=2\rangle$ $+0.9943\|M=0\rangle$

curves calculated by adding to the Hamiltonian the Zeeman term

$$H_Z = \mu_B \sum_i g_i \mathbf{B}\cdot\mathbf{s}_i, \tag{6}$$

in which, according to magnetization and HF-EPR results, an isotropic $g=2$ value can be assumed.[4]

Two different contributions have been taken into account, $C=C_{\rm ph}+C_{\rm magn}$. The magnetic contribution $C_{\rm magn}/R\beta^2$ ($\beta^{-1}=k_BT$) can be calculated from the known set of energy levels E_i,

$$\frac{\Sigma_i E_i^2 \exp(-\beta E_i)\Sigma_i \exp(-\beta E_i) - [\Sigma_i E_i \exp(-\beta E_i)]^2}{[\Sigma_i \exp(-\beta E_i)]^2}, \tag{7}$$

whereas the lattice contribution $C_{\rm ph}$ (in R units) is given by

$$C_{\rm ph}/R = \frac{234 r T^3}{(\Theta_D + \delta T^2)^3}, \tag{8}$$

where r is the number of atoms per molecule, $\Theta_D=169$ K, and $\delta=0.34$ K^{-1} accounts for the temperature dependence of the Debye temperature. The excellent agreement between experimental and calculated curves lends support to the proposed model. The energy levels as a function of the applied magnetic field are reported in Fig. 8.

In Ref. 4, measurements of relaxation, ac susceptibility, and hysteresis loops are reported. These measurements show that below 0.2 K, the magnetic relaxation time in Fe_4-thme approaches a temperature-independent value, revealing that the system enters a quantum tunneling regime, while in the thermally activated regime a barrier for the reversal of mag-

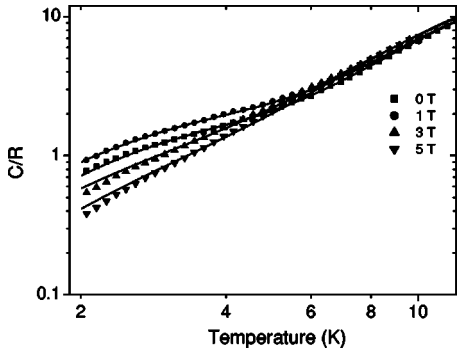

FIG. 7. Molar specific heat of Fe_4-thme molecular cluster as a function of temperature, in the presence of a magnetic field with amplitude varying from 0 to 5 T.

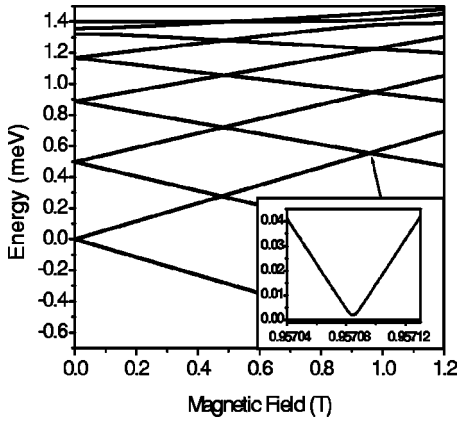

FIG. 8. Lowest energy levels of Fe_4-thme molecular cluster as a function of the applied magnetic field. The field is parallel to the easy axis. The inset evidences the region where the first anticrossing would occur if $B_4^3=0$ (the energy difference between the levels participating in the anticrossing is shown).

netization of about 15.6 K has been extracted. Besides, the steplike behavior of the measured hysteresis loops reveals that the field-dependent relaxation time $\tau(B)$ has minima at $B\sim 0$, 0.5, and 1 T. Being characterized by a small Hilbert space (the dimension is only 1296) and by a single isomer, Fe_4-thme is one of the best candidates for improving the present knowledge on QTM. The relaxation rate in the purely quantum regime depends crucially on the value of the so-called tunnel splitting Δ, i.e., the gap between the two lowest quasidegenerate states (approximately given by $|S=5, M=\pm 5\rangle$). This quantity directly reflects the in-plane anisotropy, since it would be exactly zero if only axial terms were present in H_{ZFS}. Therefore, a determination of the nonaxial term is mandatory in order to obtain a deep understanding of QTM. By considering only the D_3 symmetry-allowed B_4^3 term, Δ is zero since $|S=5, M=\pm 5\rangle$ are not connected by any power of O_4^3. On the contrary, if the B_2^2 parameter determined in this work (1.2 μeV) is added to the Hamiltonian, the tunnel splitting is nonzero and ranges from 4.7×10^{-7} μeV to about 10^{-4} μeV (if $|B_4^3|$ ranges from zero to the maximum value compatible with INS data).[17]

At $T>\sim 1.5$ K, the relaxation process in Fe_4-thme is mainly determined by interactions of the spin degrees of freedom of each molecule with the crystal phonon heat bath, resulting in an Arrhenius behavior with a barrier of about 15.6 K. Since the two lowest excited manifolds lie at about 66 K, this behavior may be understood by considering the ground $S=5$ multiplet only. The modulation of the local crystal fields $\Sigma_i\Sigma_{k,q} b_k^q(i) O_k^q(\mathbf{s}_i)$ due to elastic waves leads to the following spin-phonon coupling potential:

$$V=\sum_{\Gamma,r} B(\Gamma) O_{\Gamma r}(\mathbf{S})\epsilon_{\Gamma r}, \tag{9}$$

where Γ labels point-group representations and r is the degeneracy index. $\epsilon_{\Gamma r}$ are symmetrized strains at the cluster site (obtained by grouping the components of the local strain tensor to form irreducible representations of the point group). $O_{\Gamma r}(\mathbf{S})=\Sigma_q \alpha_{\Gamma r}(q) O_2^q(\mathbf{S})$ are symmetry-adapted quadrupolar operators obtained as appropriate linear combinations of Stevens operator equivalents. $B(\Gamma)$ is a coupling constant. For the sake of simplicity, we assumed $V\propto S_zS_x+S_xS_z$. In fact, we have verified that the addition of further terms in the spin-phonon coupling potential does not change appreciably the calculated behavior of $\tau(T)$, apart from a trivial renormalization of the spin-phonon coupling constant(s).

In a master-equation formalism,[18] the density matrix describing spin degrees of freedom satisfies

$$\dot{\rho}(t)_{mm}=\sum_{n\neq m}\rho(t)_{nn}W_{mn}-\rho(t)_{mm}\sum_{n\neq m}W_{nm}, \tag{10}$$

where $\rho(t)_{m'm}=\langle m'|\rho(t)|m\rangle$, and W_{mn} is the probability per unit time that a transition between levels $|n\rangle$ and $|m\rangle$ is induced by the interaction with phonons. The latter may be calculated by perturbation theory,

$$W_{mn}=A\pi|\langle n|S_zS_x+S_xS_z|m\rangle|^2\Delta_{mn}^3 n(\Delta_{mn}), \tag{11}$$

with

$$n(x)=(e^{\beta\hbar x}-1)^{-1},\quad \Delta_{mn}=(E_m-E_n)/\hbar.$$

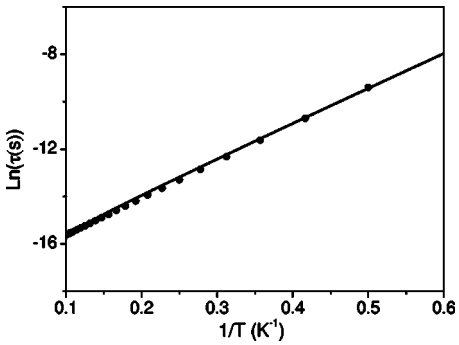

FIG. 9. Calculated temperature dependence of the relaxation time τ of the magnetization. In the range $1.5<T<10$ K, τ follows an Arrhenius behavior characterized by a barrier $U=15.6$ K (Ref. 19). Points represent a simulated Arrhenius law with $U=15.6$ K.

By solving the above equations, it is possible to calculate the time evolution of the magnetization $M(t)$. It turns out that in the temperature range $1.5<T<10$ K, the relaxation of M is exponential and characterized by a single decaying time $\tau(T)$. Moreover, in this temperature range, $\tau(T)$ follows an exponential behavior $\tau(T)=\tau_0\exp(U/k_BT)$. The parameter A, which measures the amount of spin-phonon coupling, can be fixed to 1.5×10^{-6} $(\mathrm{THz})^{-2}$ by imposing, for example, $\tau(4\ \mathrm{K})=1.7\times 10^{-6}$ s. The results are shown in Fig. 9. The calculated energy barrier $U\sim 15.6$ K is in excellent agreement with experimental data. Therefore, the small amount of in-plane anisotropy ($|B_2^2/B_2^0|\sim 0.06$) allows phonon-induced transitions between states belonging to different wells, thus lowering the effective energy barrier with respect to the energy difference between the highest and lowest state of the $S=5$ multiplet (16.2 K). In addition, we have verified that the trigonal B_4^3 term has a negligible effect on U for values compatible with neutron data.

At last, we would like to comment on the finite-field minima observed in field-dependent relaxation time $\tau(B)$ at $B\sim 0.5$ and 1 T. These minima reflect the occurrence of particularly efficient tunneling paths at these specific values of the field. Figure 8 shows that level (anti)crossings occur at 0.5 and 1 T. While anticrossings (ACs) provide a shortcut for the tunneling process and produce therefore a minimum in $\tau(B)$, no effect on $\tau(B)$ is expected from a crossing. Interestingly, while at $B\sim 1$ T sizeable ACs are produced by the above-determined rhombic term B_2^2, this term is ineffective on the crossings at $B\sim 0.5$ T, since these involve levels nonconnected by powers of $O_2^2(\mathbf{S})$. On the contrary, the trigonal B_4^3 term, which has not been detected in INS spectra, very efficiently turns these latter crossings into ACs. Thus, the minimum observed in $\tau(B)$ at $B\sim 0.5$ T demonstrates that, although B_4^3 is too small to produce visible effects in the high-frequency dynamics probed by INS, this term cannot be zero and qualitatively modifies the low-frequency dynamics which governs tunneling.

IV. CONCLUSIONS

Inter- and intra-multiplet transitions in the new Fe_4-thme compound have been measured with inelastic neutron scat-

tering. High-resolution data allowed a precise determination of the quasiaxial magnetic anisotropy. The axial-anisotropy parameter B_2^0 is increased by more than a factor of 2 with respect to the parent compound Fe_4-OMe. A nonzero second-order in-plane anisotropy term (B_2^2) is necessary in order to reproduce low-energy INS data corresponding to transitions between the highest states of the ground $S=5$ multiplet. This term, which is forbidden in D_3 symmetry, plays a crucial role in determining the tunnel splitting of Fe_4-thme. The Q dependence of the observed peaks is in very good agreement with calculations. The positions of the lowest excited manifolds confirm the values of the exchange constants deduced by fitting magnetic susceptibility. In addition, the width of the peak corresponding to $S=5\rightarrow S=4$ transitions allows us to conclude that the symmetry lowering, occurring at low temperature, does not appreciably affect exchange constants. The temperature and magnetic field dependence of the measured Schottky anomaly in the specific heat confirm the Hamiltonian deduced from the analysis of neutron data. Finally, a master-equation approach has allowed the calculation of the temperature dependence of the relaxation time $\tau\,(T)$ of the magnetization. An Arrhenius behavior with a barrier of 15.6 K has been found for $1.5<T<10$ K, in excellent agreement with experimental data.

ACKNOWLEDGMENTS

This work was partly supported by Ministero dell'Università e della Ricerca Scientifica e Tecnologica, FIRB Project. We thank M. Affronte for the helpful discussions, and the Institut Laue Langevin for access to the neutron beam facility.

[1] R. Sessoli, D. Gatteschi, A. Caneschi, and M. A. Novak, Nature (London) **365**, 141 (1993).
[2] S. Carretta, E. Liviotti, N. Magnani, P. Santini, and G. Amoretti, Phys. Rev. Lett. **92**, 207205 (2004).
[3] D. Gatteschi and R. Sessoli, Angew. Chem., Int. Ed. **42**, 268 (2003), and references therein.
[4] A. Cornia, A. C. Fabretti, P. Garrisi, C. Mortalò, D. Bonacchi, D. Gatteschi, R. Sessoli, L. Sorace, W. Wernsdorfer, and A.-L. Barra, Angew. Chem., Int. Ed. **43**, 1136 (2004).
[5] A. Bouwen, A. Caneschi, D. Gatteschi, E. Goovaerts, D. Schoemaker, L. Sorace, and M. Stefan, J. Phys. Chem. B **105**, 2658 (2001).
[6] T. C. Schwendemann, P. S. May, M. T. Berry, Y. Hou, and C. Y. Meyers, J. Phys. Chem. A **102**, 8690 (1998).
[7] R. Adams and E. W. Adams, Org. Synth. Coll. **1**, 459 (1941).
[8] G. A. Hill and E. W. Flosdorf, Org. Synth. Coll. **1**, 462 (1941).
[9] L. T. Sandborn and E. W. Bousquet, Org. Synth. Coll. **1**, 526 (1941).
[10] B. S. Furniss, A. J. Hannaford, P. W. G. Smith, and A. R. Tatchell, *Vogel's Textbook of Practical Organic Chemistry*, 5th ed. (Longman Scientific & Technical, New York, 1989).
[11] K. R. Kopecki, D. Nonhebel, G. Morris, and G. S. Hammond, J. Org. Chem. **27**, 1036 (1962).
[12] T. Guidi, G. Amoretti, R. Caciuffo, S. Carretta, A. Cornia, C. D. Frost, and E. Liviotti, J. Magn. Magn. Mater. **272–276**, 777 (2004).
[13] A. Abragam and B. Bleaney, *Electron Paramagnetic Resonance of Transition Ions* (Clarendon Press, Oxford, 1970).
[14] R. Caciuffo, G. Amoretti, A. Murani, R. Sessoli, A. Caneschi, and D. Gatteschi, Phys. Rev. Lett. **81**, 4744 (1998).
[15] J. J. Borras-Almenar, J. M. Clemente-Juan, E. Coronado, and B. S. Tsukerblat, Inorg. Chem. **38**, 6081 (1999).
[16] G. Amoretti, S. Carretta, R. Caciuffo, H. Casalta, A. Cornia, M. Affronte, and D. Gatteschi, Phys. Rev. B **64**, 104403 (2001).
[17] When $B_2^2\neq 0$, the tunnel splitting is remarkably influenced by the value of B_4^3 since the contemporary presence of O_2^2 and O_4^3 in the Hamiltonian opens highly efficient tunneling pathways.
[18] K. Blum, *Density Matrix Theory and Applications* (Plenum Press, New York, 1996); P. Politi, A. Rettori, F. Hartmann-Boutronn, and J. Villain, Phys. Rev. Lett. **75**, 537 (1995).
[19] A small static field of 20 mT has been added in order to take into account dipolar interactions between different clusters.